Supporting Information

# A Tricky Water Molecule Coordinated to a Verdazyl Radical-Iron(II) Complex: a Multitechnique Approach.

*Hajime Kamebuchi,[1] Masashi Okubo,[2] Atsushi Okazawa,[1] Masaya Enomoto,[3] Jun Harada,[1] Keiichiro Ogawa,[1] Goro Maruta,[4] Sadamu Takeda,[4] Norimichi Kojima*,[1] Cyrille Train,*,[5] and Michel Verdaguer[6]*

[1]Graduate School of Arts and Sciences, The University of Tokyo, Komaba 3-8-1, Meguro-ku, Tokyo 153-8902, Japan. [2]National Institute of Advanced Industrial Science and Technology, Umezono 1-1-1, Tsukuba, Ibaraki 305-8568, Japan. [3]Department of Chemistry, Faculty of Science Division I, Tokyo University of Science, Kagurazaka 1-3, Shinjuku-ku, Tokyo 162-8601, Japan. [4]Department of Chemistry, Faculty of Science, Hokkaido University, Kita 10, Nishi 8, Sapporo 060-0810, Japan [5]Laboratoire National des Champs Magnétiques Intenses, UPR CNRS 3228, 25 rue des Martyrs, B.P. 166, 38042, Grenoble Cedex 9, France; Université Joseph Fourier, BP 53, F-38041 Grenoble Cedex 9, France. [6]Institut Parisien de Chimie Moléculaire, Université Pierre et Marie Curie-Paris 6, UMR CNRS 7201, F-75252, Paris, France.

## Table of Contents

Table S1. Selected Crystallographic Data for **2** at 300 K and 90 K.

| compound | | **2** |
|---|---|---|
| formula | | $C_{10}H_{12}D_8FeN_8O_{10}$ |
| formula weight | | 476.21 |
| crystal system | | triclinic |
| space group | | *P*-1 |
| *a*/Å | 9.1722(7) | 9.1747(6) |
| *b*/Å | 9.5972(7) | 9.2567(6) |
| *c*/Å | 10.5527(8) | 10.6372(7) |
| $\alpha$/deg | 84.837(2) | 84.2890(10) |
| $\beta$/deg | 83.709(2) | 84.4090(10) |
| $\gamma$/deg | 80.095(2) | 79.2460(10) |
| *V*/Å$^3$ | 907.17(12) | 880.24(10) |
| *Z* | 2 | 2 |
| $R_1$ ($I > 2\sigma(I)$) | 0.0408 | 0.0341 |
| $wR_2$ (all data) | 0.1206 | 0.0911 |
| G.O.F. | 1.045 | 1.073 |
| *T*/K | 300 | 90 |

Table S2. Distances around the Fe atoms in **1**(RT) compared with Co and Ni derivatives

| *Distances / Å* | *Fe (this work)* | *Co [7]* | *Ni [7]* |
|---|---|---|---|
| MO1($H_2O$) | 2.069 | 2.023 | 2.037 |
| MO2($H_2O$) | 2.121 | 2.060 | 2.097 |
| MO3(vd) | 2.098 | 2.035 | 2.055 |
| MO6(vd) | 2.092 | 2.025 | 2.043 |
| MN1(vd) | 2.208 | 2.127 | 2.185 |
| MN5(vd) | 2.213 | 2.141 | 2.192 |

Table S3. Temperature Dependence of Mössbauer Parameters for **2**.

| $T$ (K) | $\delta$ (mm s$^{-1}$) | | $\Delta E_Q$ (mm s$^{-1}$) | | $\Gamma$ (mm s$^{-1}$) | | Relative area | |
|---|---|---|---|---|---|---|---|---|
| | HT | LT | HT | LT | HT | LT | HT | LT |
| 300 | 1.096 | 1.139 | 1.328 | 1.968 | 0.290 | 0.390 | 0.742 | 0.258 |
| 250 | 1.137 | 1.180 | 1.364 | 2.012 | 0.418 | 0.503 | 0.707 | 0.293 |
| 200 | 1.174 | 1.228 | 1.440 | 2.302 | 0.447 | 0.595 | 0.673 | 0.327 |
| 150 | 1.181 | 1.221 | 1.497 | 2.470 | 0.487 | 0.577 | 0.630 | 0.370 |
| 100 | 1.224 | 1.250 | 1.609 | 2.720 | 0.493 | 0.573 | 0.530 | 0.470 |
| 90 | 1.228 | 1.257 | 1.676 | 2.762 | 0.578 | 0.620 | 0.514 | 0.486 |
| 80 | 1.238 | 1.270 | 1.688 | 2.819 | 0.548 | 0.559 | 0.487 | 0.513 |
| 70 | 1.240 | 1.269 | 1.725 | 2.858 | 0.545 | 0.540 | 0.446 | 0.554 |
| 60 | 1.247 | 1.272 | 1.816 | 2.917 | 0.570 | 0.493 | 0.428 | 0.572 |
| 50 | 1.227 | 1.244 | 1.950 | 2.973 | 0.613 | 0.507 | 0.383 | 0.617 |
| 40 | 1.259 | 1.271 | 2.121 | 3.020 | 0.640 | 0.457 | 0.361 | 0.639 |
| 30 | 1.250 | 1.250 | 2.063 | 3.045 | 0.582 | 0.409 | 0.291 | 0.709 |
| 20 | 1.313 | 1.250 | 2.357 | 3.143 | 0.511 | 0.465 | 0.202 | 0.798 |
| 10 | 1.313 | 1.250 | 2.652 | 3.143 | 0.572 | 0.456 | 0.122 | 0.878 |

$\delta$: Isomer shift, $\Delta E_Q$: Quadrupole splitting, $\Gamma$: Line width, HT: Predominant species at high temperature, LT: Predominant species at low temperature.

Table S4a Experimental J values ($\boldsymbol{H} = -J_{ij}\boldsymbol{S}_i\boldsymbol{S}_j$)

| *J / cm$^{-1}$* | $J_{M\text{-}rad}$ | $J_{rad\text{-}rad}$ | *Ref.* |
|---|---|---|---|
| Fe(II) | -27.1 | -42.8 | this work |
| Co(II) | +68 | -42 | [7] |
| Ni(II) | +188 | -38 | [7] |

Table S4b Equations for the analysis of the magnetic data using Eqn (3)

| *Metal ion* | $J_{M\text{-}rad}$ | *Eqn number* |
|---|---|---|
| Fe | $(1/2)\,[j_{t2g-p^*} + j_{eg^*-p^*}]$ | (3.1) |
| Co | $(1/3)\,[j_{t2g-p^*} + 2j_{eg^*-p^*}]$ | (3.2) |
| Ni | $j_{eg^*-p^*}$ | (3.3) |

Table S4c Computation of $j_{t2g-p^*}$ assuming $j_{eg^*-p^*} = 188$ cm$^{-1}$ calculated from eqn. (3.3) is metal-independent

| *Set of equations* | $j_{t2g-p^*}$ |
|---|---|
| (3.1) and (3.2) | -312.4 cm$^{-1}$ |
| (3.2) and (3.3) | -172 cm$^{-1}$ |
| (3.3) and (3.1) | -242 cm$^{-1}$ |

(b)

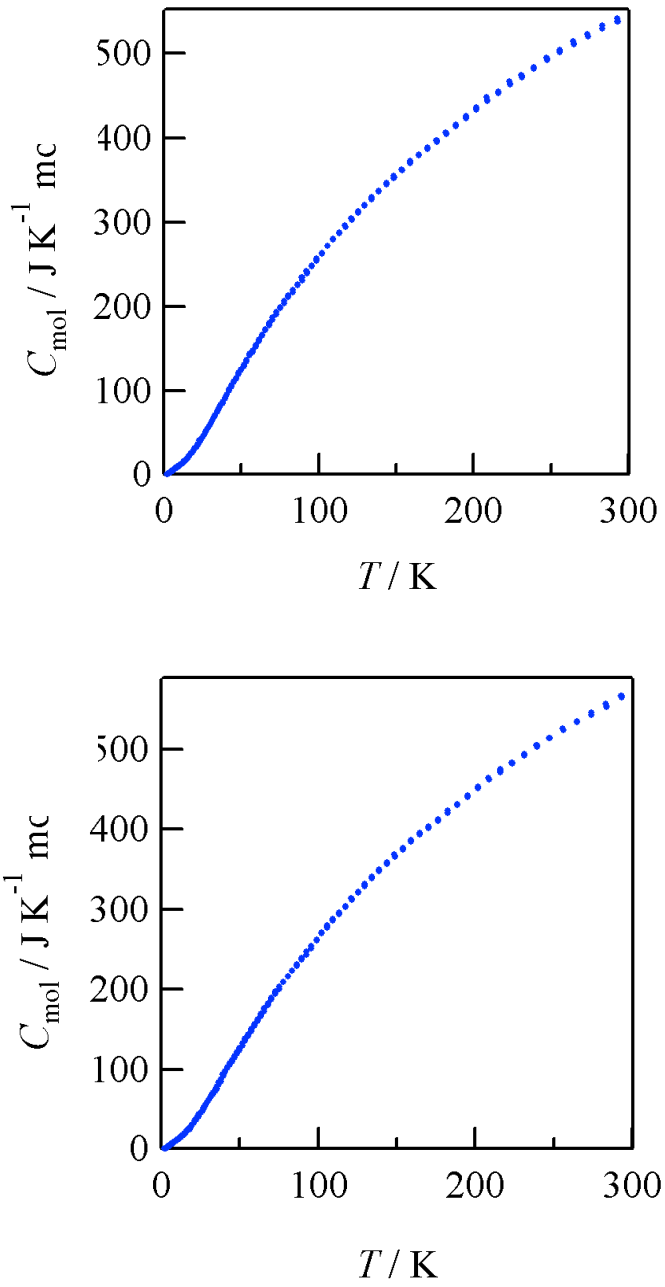


Figure S1. Temperature dependence of molar heat capacity measured by relaxation method. (a) **1**, (b) **2**.

b)

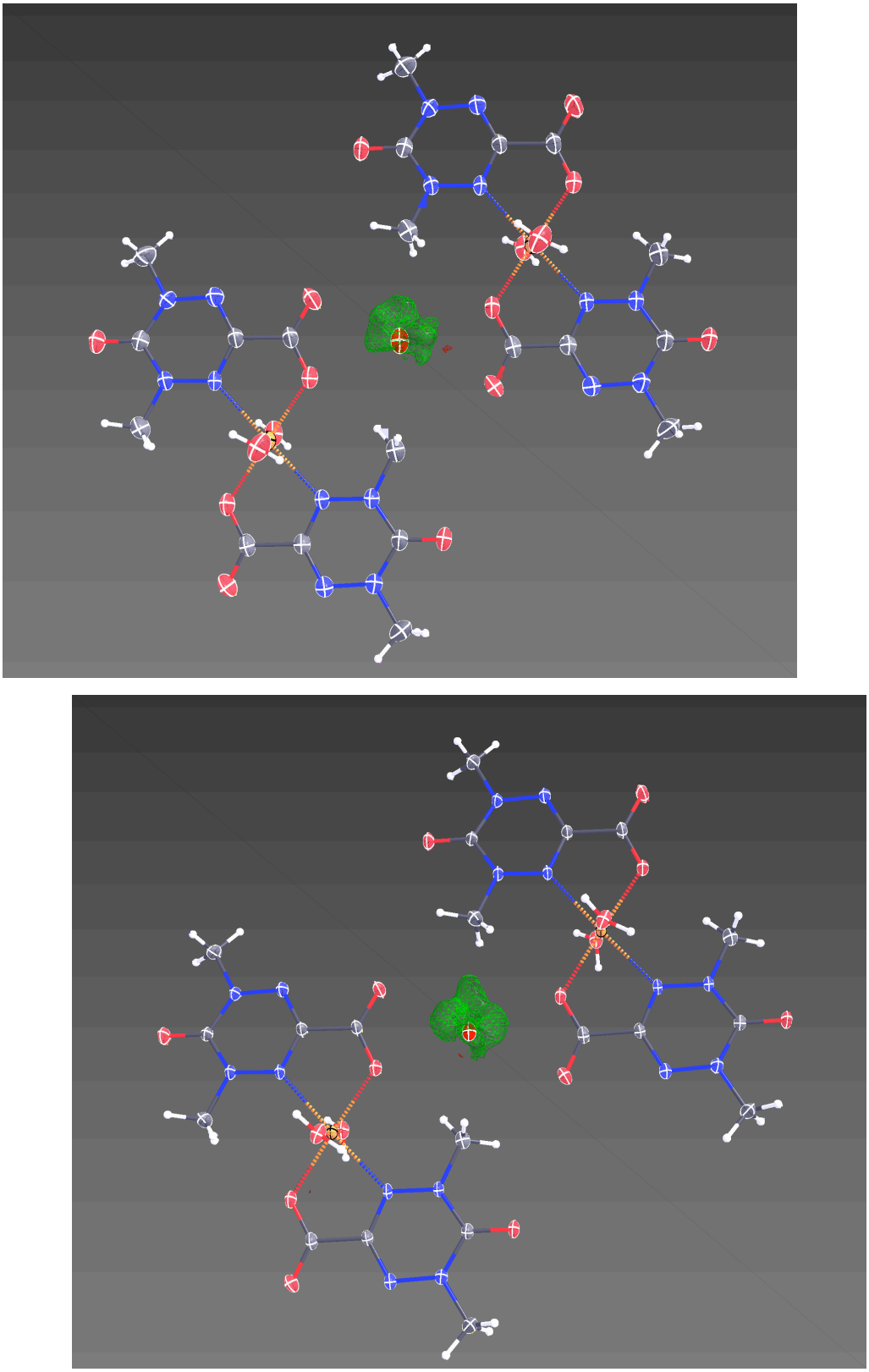

Figure S2. Electron density difference map for hydrogen atoms of coordinated water II (around O2) in **1** at (a) 300 K and (b) 90 K.

b)

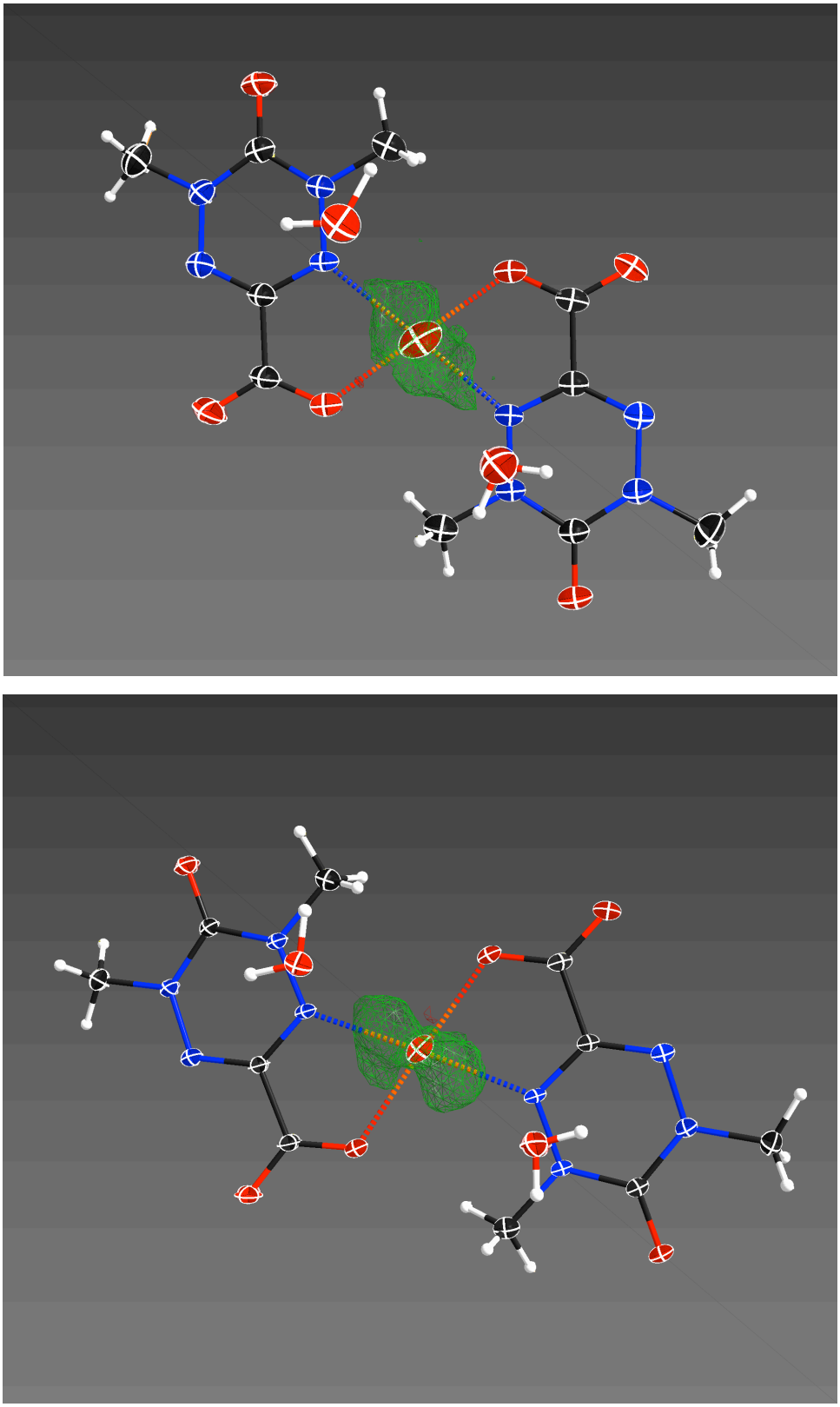

Figure S3. Electron density difference map for hydrogen atoms of the coordinated water I (around O1) in **1** at (a) 300 K and (b) 90 K.

b)

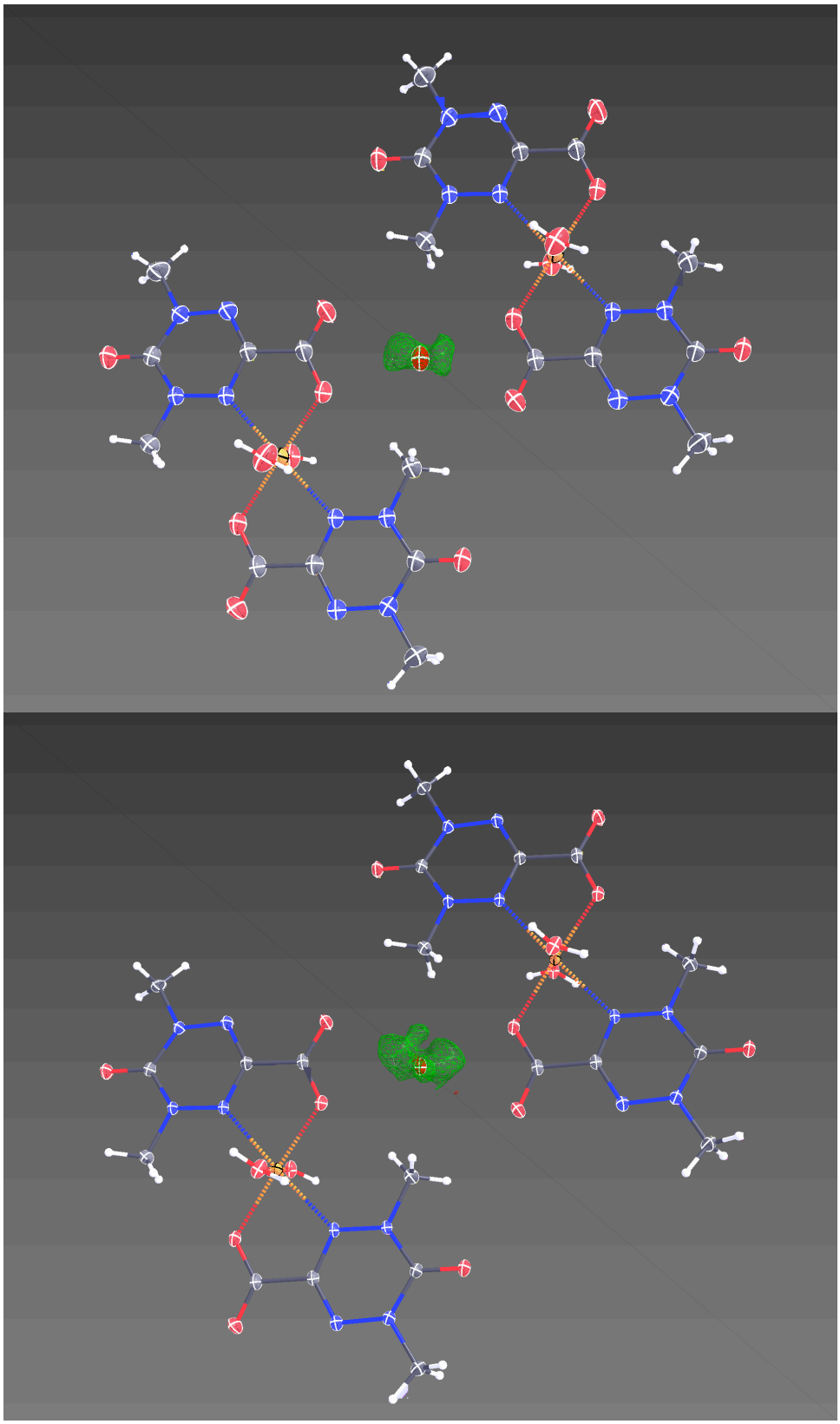

Figure S4. Electron density difference map for deuterium atoms of the coordinated water II (around O2) in **2** at (a) 300 K and (b) 90 K.

b)

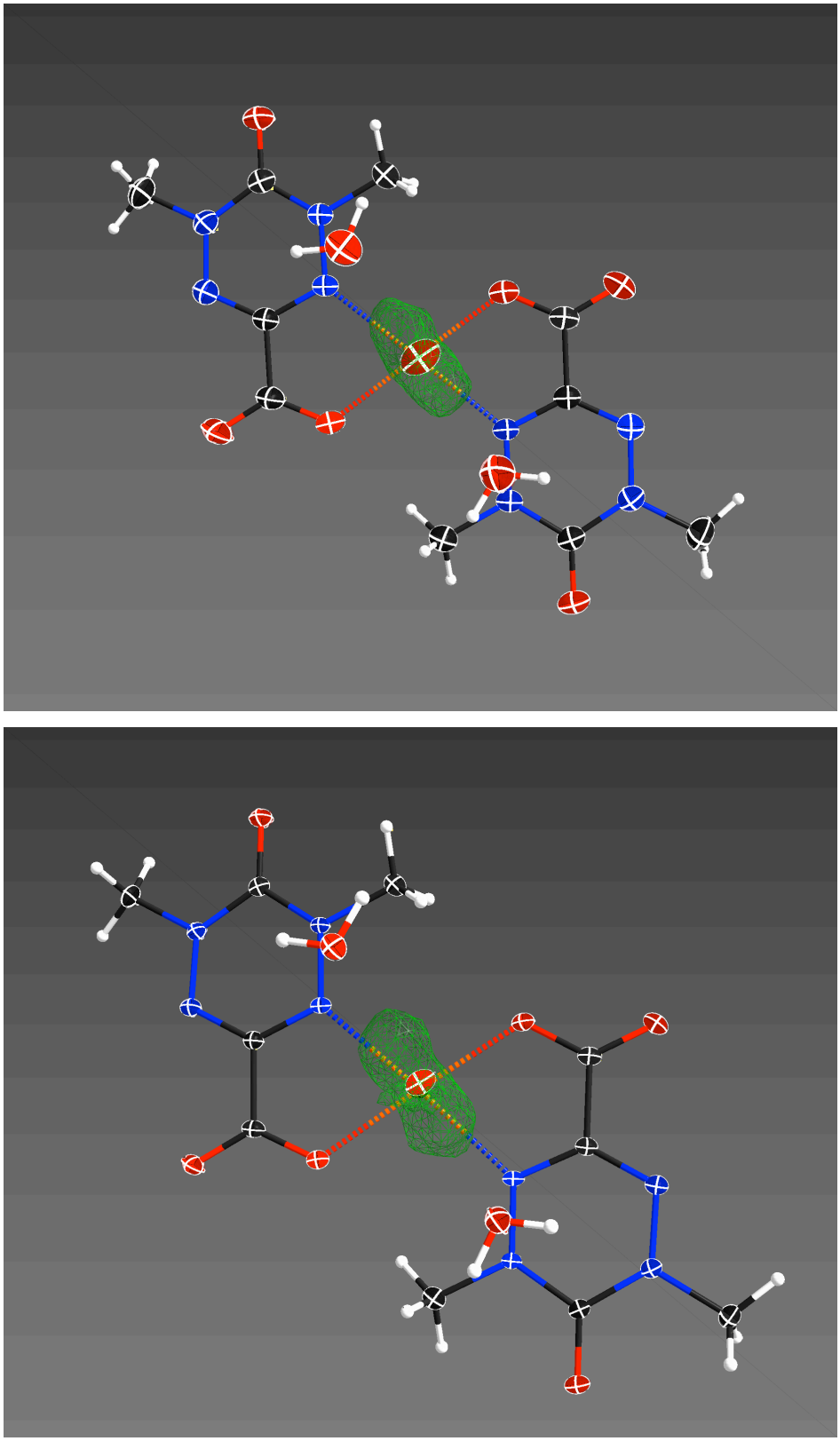

Figure S5. Electron density difference map for deuterium atoms of the coordinated water I (around O1) in **2** at (a) 300 K and (b) 90 K.

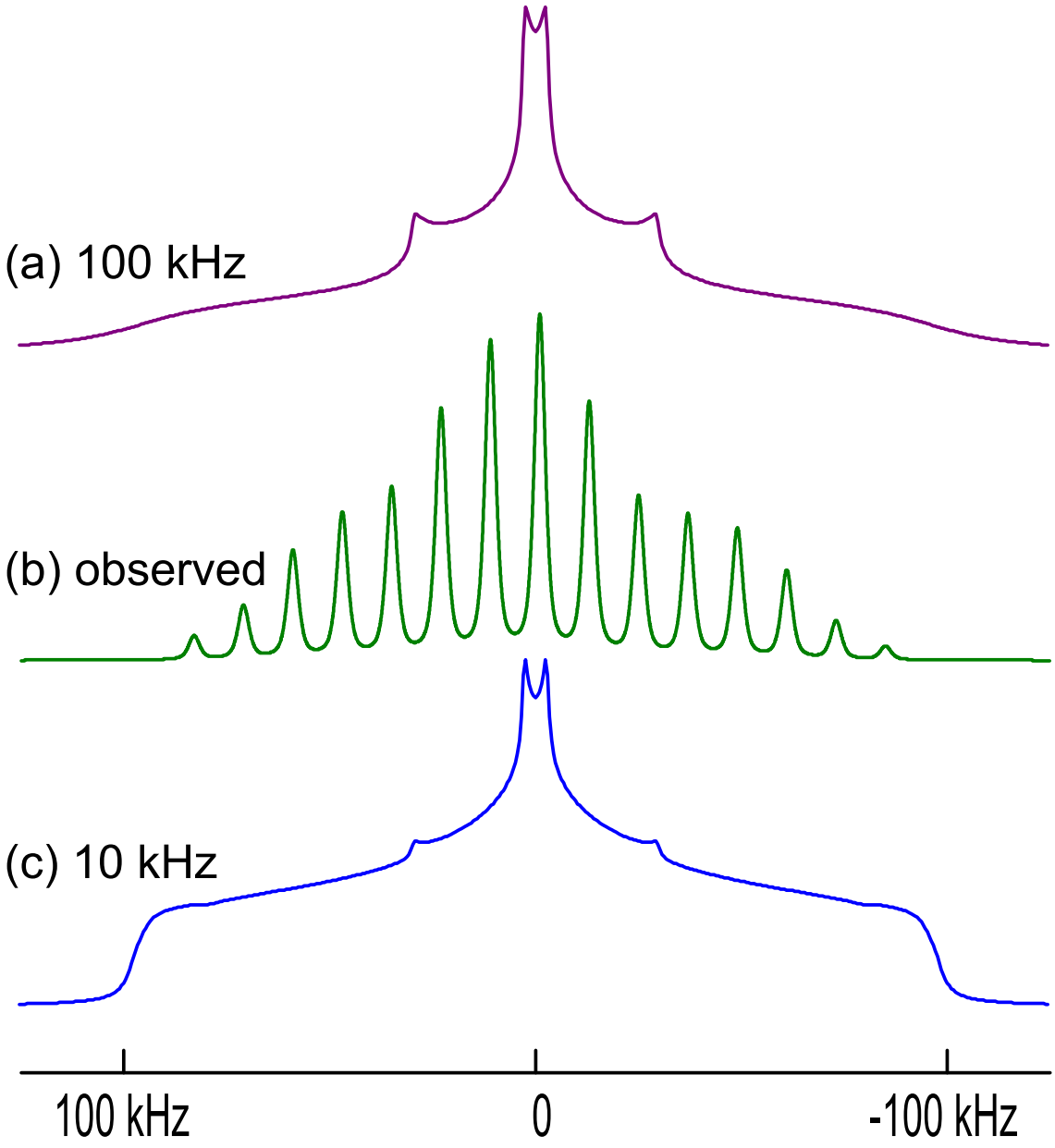


Figure S6. Observed MAS D-NMR spectrum of **2** (b) and simulations of static powder pattern based on the condition that coordinated water II undergoes a slow two-site jump, (a) 100 kHz, (c) 10 kHz, in addition to a 180 degree flip-flop jump in the first limit (100MHz). Angle for the slow two-site jump was set to 73 degree, which was estimated from X-ray diffraction experiment. Quadrupole coupling constant Cq = 243.5 kHz for typical water molecule was used.